

Calculation of the Axial Charge of a Heavy Nucleon in Lattice QCD

by

Dimitra Anastasia Pefkou

Submitted to the Department of Physics
in partial fulfillment of the requirements for the degree of

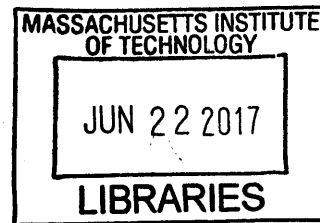
Bachelor of Science in Physics

at the

MASSACHUSETTS INSTITUTE OF TECHNOLOGY

September 2016

© Massachusetts Institute of Technology 2016. All rights reserved.



ARCHIVES

Author 

Department of Physics

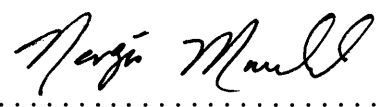
August 3, 2016

Certified by 

Dr. William Detmold

Assistant Professor

Thesis Supervisor

Accepted by 

Professor Nergis Mavalvala

Senior Thesis Coordinator, Department of Physics

Calculation of the Axial Charge of a Heavy Nucleon in Lattice QCD

by

Dimitra Anastasia Pefkou

Submitted to the Department of Physics
in partial fulfillment of the requirements for the degree of

Bachelor of Science in Physics

at the

MASSACHUSETTS INSTITUTE OF TECHNOLOGY

September 2016

© Massachusetts Institute of Technology 2016. All rights reserved.

Signature redacted

Author

|

.....

Department of Physics

August 3, 2016

Signature redacted

Certified by.

.....

Dr. William Detmold

Assistant Professor

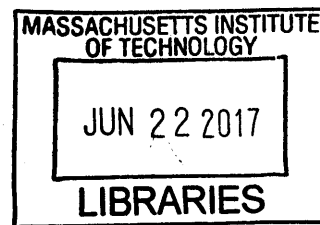
Thesis Supervisor

Signature redacted

Accepted by

Professor Nergis Mavalvala

Senior Thesis Coordinator, Department of Physics



ARCHIVES

Calculation of the Axial Charge of a Heavy Nucleon in Lattice QCD

by

Dimitra Anastasia Pefkou

Submitted to the Department of Physics
on August 3, 2016, in partial fulfillment of the
requirements for the degree of
Bachelor of Science in Physics

Abstract

In this thesis, we aim to calculate the non-renormalized axial charge g_A of a heavy nucleon made out of quarks at the physical mass of the strange quark. We present the framework of Lattice QCD which makes the calculation of such observables attainable from first principles. The data used for the estimation of g_A were obtained on a $24^3 \times 64$ hypercubic lattice with lattice spacing $a \sim 0.12 \text{ fm}$ and pion mass $m_\pi = 0.450 \text{ GeV}$. Three different source-sink separations were used, $t_{sink} = [12a, 14a, 16a]$. For each timeslice separation signal we perform a correlated χ^2 fit and obtain the following values for g_A : 0.551, 0.564 and 0.556. The unrenormalized value for g_A is extracted taking the limit as $t_{sink} \rightarrow \infty$ and is shown to be $g_A = 0.558$. We discuss how the accuracy of this result is compromised by the small number of t_{sink} values, by excited state contamination and by the increase of statistical noise with time.

Thesis Supervisor: Dr. William Detmold
Title: Assistant Professor

Acknowledgments

Foremost, I would like to thank my supervisor, Dr. William Detmold, for all the motivation, knowledge and advice he provided me while supporting my research for the past year. He was available everytime I had a question and his answers always steered me to the right direction.

I would also like to thank Dr. Phiala Shanahan, Andres Rios and Ben Elder for their generous help at different parts of this project.

I am grateful to my advisor, Dr. Isaac Chuang, for all our inspirational meetings and the creative nature that always underlied his advice.

Finally, I must thank my parents, my silbings and my friends for their unconditional trust and support throughout my studies.

Contents

1	Introduction	9
1.1	The Strong Force	9
1.2	Lattice QCD	13
1.3	Goals of Thesis	16
2	Background	17
2.1	Lagrangian Formulation of Lattice QCD	17
2.1.1	On Lagrangians and Gauge invariance	17
2.1.2	Lagrangian formulation of Quantum Chromodynamics	19
2.1.3	Lattice QCD naive action	20
2.1.4	Path integral and observables	24
2.1.5	Fermi statistics and the Wilson term	26
2.2	Hadron Structure with Lattice Methods	28
2.2.1	Elastic $ep \rightarrow ep$ scattering and the electromagnetic Form Factors	28
2.2.2	Nucleon decay and the axial Form Factors	31
2.2.3	Hadron correlators at the quark level	33
2.2.4	Extracting the form factors from hadron correlators	39
2.3	Symanzik Improvement and Renormalization	40
2.3.1	Clover term	40
2.3.2	Renormalization of naive currents	41
3	Method	43
3.1	Data Acquisition	43

3.2	Data Processing	44
4	Results	47
4.1	Effective mass	47
4.2	Raw signal of g_A	48
5	Conclusion	51
5.1	Summary of results and discussion	51
5.2	Suggestions for improvement and future projects	52

Chapter 1

Introduction

1.1 The Strong Force

The strong force was developed historically from the study of nuclei. By the 1930's, scientists were more than familiar with protons and electrons and had a deep understanding of electromagnetic interactions. However, there was no successful model that explained what keeps positively charged protons bound together in nuclei. This suggested new force was named strong force as it had to be stronger than the electromagnetic force. It also had to have a short range since it was not observed anywhere else besides within the nucleus [1].

There was also a discrepancy between the proton content of a nucleus and its mass, implying the existence of another particle. In 1932, Chadwick first discovered this particle, called neutron [2]. The neutron is slightly heavier than the proton and electrically neutral; however it interacts through the nuclear force in a very similar way as the proton. Moreover, a neutron can decay into a proton and vice versa through β decay, the second being energetically possible only inside a nucleus. These observations, as well as the analogy to isotopes in atomic physics, motivated Heisenberg to come up with the idea of isospin. He proposed that isospin is a quantity that is conserved in strong interactions; the proton and the neutron correspond to opposite z-component eigenvalues of the same isospin state [3]. That meant that the underlying symmetry behind the strong force would be an SU(2) group and all

strong interactions would have to be symmetrical under $SU(2)$ rotations. All that was missing for a complete theory was a mediator for the strong force, analogous to the photon for the electromagnetic force.

In 1934 Yukawa took into consideration the strength and short range of the nuclear force and proposed a theory for the strong force. He predicted the mass of the mediator and, since it was lighter than the nucleon (baryon) and heavier than the electron (lepton), he called it the meson. Such a particle had not been observed at the time. A few years later though, experiments revealed that cosmic rays contain such a middle-weight particle. It was initially considered a good candidate for Yukawa's meson. However, its lifetime did not match his predictions. It also interacted with nuclei very weakly, in complete disagreement with its assumed role in the strong force. In 1947 it was established that cosmic rays actually contain two types of middle-weight particles, the muon (μ) and the pion (π). Most of the pions produced in the upper atmosphere decay by the time they reach sea-level, and one of the decay products is the muon [4]. The pion's properties made it an appropriate candidate for Yukawa's meson.

In 1947 the relative completeness of Yukawa's theory was doubted after the discovery of the kaon (K^0) [5]. It was first observed to be produced from cosmic rays incident on a lead plate and it decayed as:

$$K^0 \rightarrow \pi^+ \pi^- \quad (1.1)$$

Soon afterwards several similar particles were discovered, K^+ , ρ , ϕ and others. Since they behaved like heavier pions, they were categorized as mesons. Around the same time, a new family of particles that behaved like heavier nucleons was discovered too. The first one, observed in 1950, was named Λ [6]. Its decay channel is:

$$\Lambda \rightarrow p \pi^- \quad (1.2)$$

All these new particles confused the scientific community and were rightfully named "strange" particles. One puzzling characteristic was that even though their

production was really fast (10^{-23} seconds), many of them decayed much slower (10^{-10} seconds). That implied that they were produced via the strong interaction but often decaying via the weak interaction. Many strong reactions that should not be prohibited from either baryon number conservation or meson number conservation were simply not happening. That seemed to be violating another rule, attributed to either Feynman or Gell-Mann: "Everything not forbidden is compulsory"!

To offer an explanation to that, physicists gave hadrons a new quantum number, called strangeness, and proposed that strangeness was conserved in electromagnetic and strong interactions but not necessarily conserved in weak interactions [7]. Gell-Mann and Ne'eman proposed to combine strangeness with isospin by an SU(3) group symmetry that categorized the mesons and the baryons into octets and decuplets [8].

In 1964 both Gell-Mann and Zweig independently introduced a model that explains why hadrons can be organized in such patterns [9,10]. They suggested that there exist three particles, now called up, down and strange, with charge $\frac{2}{3}$, $-\frac{1}{3}$ and $-\frac{1}{3}$ respectively, as well as their three corresponding antiparticles with opposite charge. Baryons are then bound states of three such particles (quarks), antibaryons of three antiparticles (antiquarks) and mesons and antimemesons of a quark and an antiquark. All quarks are fermions with spin $\frac{1}{2}$. In later years it was discovered that there are actually six different flavors of quarks, in analogy with the six types of leptons.

There were two most obvious problems with the quark model. The first was that no individual quarks were ever observed. The second was that the existence of the Δ^{++} baryon with quark content uuu violates Pauli's exclusion principle. To address these problems, Greenberg introduced the idea that all quarks carry one out of three possible colors, 'red', 'green' or 'blue' [11]. All bound states detected have to be colorless, which explains why quarks are not detected. Baryons and mesons contain quarks the colors of which combine to give a colorless state.

The quark model was not immediately taken seriously by the physics community. A substructure for the proton was expected since 1933, when Stern measured the proton magnetic moment to be different than what was predicted for a point-like particle [12]. In later years, deep inelastic scattering experiments (high-energy

electron-nucleon scattering) at SLAC showed that nucleons did have a substructure, and their constituents were called partons [13]. The *Gargamelle* bubble chamber results showed that the charge of the constituents were the same as those predicted by the quark model [14]. There was no clear explanation about why quarks are confined in hadrons or why they do not radiate when highly accelerated. Intuition from electromagnetism and gravity suggest that interactions are stronger at short distances. The coupling constant of the strong force seemed to be smaller at short distances, a phenomenon now called 'asymptotic freedom'.

In 1973, Gross, Wilczek and Politzer showed that certain types of gauge theories demonstrate asymptotic freedom. Their proposed theory of the strong force is called Quantum Chromodynamics (QCD) and it demonstrates asymptotic freedom as long as $11N_c > 2N_f$, where N_c is the number of colors and N_f is the number of flavors [15,16]. This is consistent with the experimental evidence of 3 colors and six flavors in strong interactions. QCD demonstrates SU(3) group symmetry in color space. Note that this differs from the earlier proposed SU(3) group in flavor space. The mediators of the strong force in QCD are bosonic particles called gluons. In contrast to the uncharged photons, gluons carry two color indices which make self-interactions possible. In this theory, quarks interact with each other via gluon fields. In order to increase the separation between them, one needs to do work which is stored as potential energy. As the distance increases, the energy needed increases too, making it more energetically favorable to create quark-antiquark pairs out of vacuum and make more bound hadronic states instead of separating the quarks.

Multiple experiments have supported QCD as a candidate theory for strong interactions, like the discoveries of the charm [18], bottom [19] and top [20] quarks and the discovery of quark jets [21]. Another example is the agreement of the measurements of the coupling constant α_s from the LEP and the DIS experiments [22]. The two kinds of experiments involve different processes but they take place in the same energy scale. Figure 1-1 presents experimental data verifying the running of the coupling constant α_s in different energy regimes.

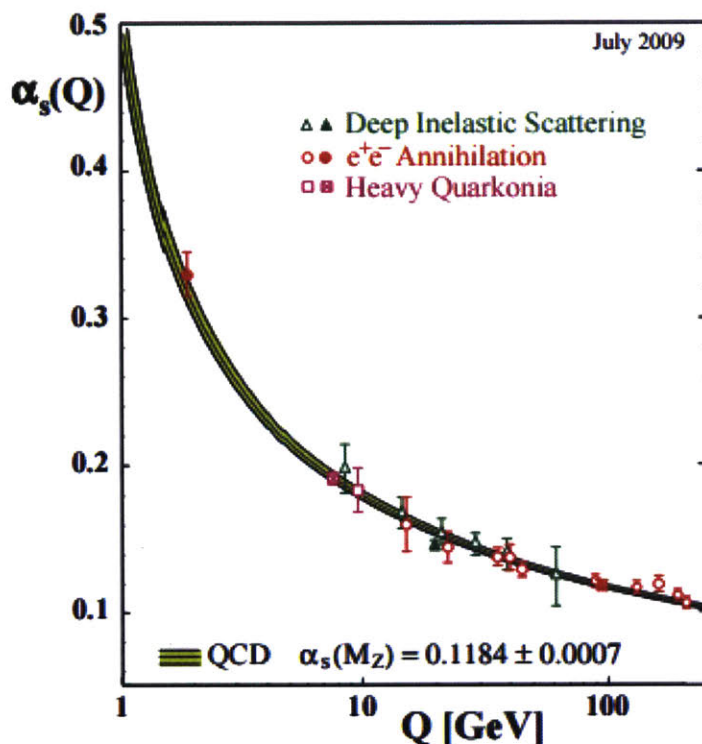


Figure 1-1: Measurements of α_s as a function of the energy scale Q . The curve is the QCD prediction of the running of α_s [17].

1.2 Lattice QCD

Part of the complexity of QCD calculations lays in the fact that the running of the coupling constant requires different approaches to be adopted for different energy regimes. Bound hadronic states are associated with lower energies, where the nature of the strong interaction is non-perturbative, something that follows from asymptotic freedom. QCD calculations in that regime are not dealing with elementary point-like particles, but with composite hadrons. Their constituents interact via gluonic fields, which carry two color indices and are therefore matrices in color space, making computations of hadronic observables particularly challenging.

In 1974, Wilson introduced a method that would allow such calculations to be made, called Lattice QCD [23]. Lattice QCD is a discrete gauge theory, with its lagrangian defined on a 4-dimensional hypercubic lattice. The fermionic quark fields of QCD are placed on the sites of the lattice and the gluon fields are matrices as-

signed as the links connecting neighbouring lattice sites. The discretization allows to make calculations of hadronic quantities from first principles and extrapolate to the physical quantities by taking the limit where the volume of the lattice is infinite and the lattice spacing is zero. These quantities are expressed using a lattice path integral formulation, as it will be explained in Chapter 2. For the size of a lattice used in actual calculations, the integrals over gluonic fields are too many to perform deterministically. For that reason, they are build through Markov chain processes and importance sampling is used to correctly weigh the probability of each configuration. These calculations are intensive and require petaflops of supercomputing power [24].

The kinds of observables that most of lattice calculations focus on are related with current experimental projects, like the scattering of electrons with hadrons through the the electromagnetic force and the weak interactions of hadrons. When hadrons interact with the respective currents, the vector and the axial vector, their behavior deviates from that of point-like particles. Studying the dependencies of the scattering amplitude on quantities like the energy, polarization and momentum experimentally makes it possible to relate the two through quantities called the form factors. The form factors contain information on the structure of hadrons and one can use them to extract unknown quantities like the charge distribution, the charge radius, the magnetic spin and tha axial charge radius. The same dependencies can be derived from first principle Lattice QCD calculations and, with the help of the path integral formulation, one can access the same unknown quantities through lattice simulations [25].

The conservation of the vector current and the axial vector current correspond to two important symmetries of QCD: the isospin symmetry and the chiral symmetry. The isospin symmetry requires that the up quark and the down quark have the same mass, a valid assumption in hadronic physics. Chirality requires that the mass of quarks is zero. The mass of hadrons is much larger that that of the two lightest quarks, which makes chirality an approximate symmetry in hadronic physics. Chiral symmetry is spontaneously broken in strong interactions, which means that while the Hamiltonian pocesses the symmetry, the ground state does not. The Goldstone

bosons of chirality are the pions, which acquire mass with the spontaneous breaking. In the low energy regime, pions dominate hadronic interactions and it is possible to express observables in terms of pion properties [26]. One example is the axial vector charge g_A , which in the chiral limit can be written as:

$$g_A = \frac{f_\pi g_{\pi NN}}{m_N} \quad (1.3)$$

where f_π is the decay constant of the pion, $g_{\pi NN}$ the pion-nucleon coupling constant and m_N the mass of the nucleon. Eq. 1.3 is also known as the Goldberger-Treiman relation [27].

Lattice methods have evolved a lot in the past decades through the improvement of algorithms and the increase of computational power. They have been successful in calculating benchmark observables of the nucleon and the pion, like their masses and axial charges [28]. These calculations, done from first principles, can be directly compared with experimental results to test for consistency and provide evidence for the validity of QCD in low energy scales, just like DIS experiments did for high energy scales. They can also be used to predict quantities not yet observed experimentally and thus contribute to the planning of future experiments, but also reveal information on the nature of hadrons that are unstable and particularly hard to observe in experiments. Lattice groups around the world are collaborating to solve problems like the experimental inconsistency between separate measurements of the proton radius, known as the proton radius puzzle. Another problem that might be solvable through lattice techniques is calculating how much of the $\frac{1}{2}$ spin of the nucleon is carried by quarks and how much by gluons.

There are a number of subtleties and limitations in the setting up of lattice calculations. The finite lattice size provides with an ultraviolet cut-off since it dictates which energies are available, but it also creates unphysical terms with a dependency on the size of the lattice. This can be dealt with by making calculations for different lattice sizes and extrapolating to zero. Most hadron ground state structure measurements require a very large time, however signal to noise ratio increases with time.

Moreover at lower times there is more contamination by excited states. Therefore one needs to carefully tune the time parameters in order to get reasonable results. Last, the finite volume of the lattice makes it hard to make calculations at masses as low as the physical ones ($m_\pi = 0.135 \text{ GeV}$). The spatial size of the lattice box must be much larger than the Compton wavelength of the pion, m_π^{-1} , to account for the effects of the pion cloud in the hadron structure [29]. However there have been significant improvements and many projects today use physical mass configurations in their simulations.

1.3 Goals of Thesis

In this project we will focus on a heavy version of the nucleon, with its constituent quarks having the physical mass of strange quarks instead of the light u and d quarks. We will attempt to estimate its axial charge, g_A . The axial charge is of crucial importance as it dictates how hadrons couple with the axial vector current. It is also a measure of the spontaneous chiral symmetry breaking in the low energy regime. A good understanding of the axial charge is essential for the future of experiments taking place at SLAC and at the LHC. The current experimental result for the axial charge is $g_A = 1.26(95)$.

Through a large sample of gauge field configurations on a $24^3 \times 64$ sized lattice and the consideration of three time separations we aim to give a statistical approximation of the non-renormalized heavy nucleon axial charge. We also aim to carefully consider the effects that excited state contamination and finite volume effects have on the accuracy of the result.

Chapter 2

Background

In the beginning of this chapter, we will outline the theoretical formulation and algebraic tools of Lattice Quantum Chromodynamics. This is only a brief review and serves the purpose of demonstrating how Lattice calculations are built. For a more complete review of each section, we refer the reader to the corresponding chapters of Gattringer & Lang's *Quantum Chromodynamics on the Lattice: An Introductory Presentation*.

2.1 Lagrangian Formulation of Lattice QCD

2.1.1 On Lagrangians and Gauge invariance

In classical mechanics, an alternative to applying Newton's laws is the Lagrangian formulation. One can define the Lagrangian as:

$$L(x, v) = \frac{1}{2}mv^2 - U(x) \tag{2.1}$$

where m is the mass of the object, v is its velocity and $U(x)$ is the potential. The action is defined as:

$$S = \int_{t_1}^{t_2} dt L(x, v) \tag{2.2}$$

The equations of motion are recovered by taking $\delta S = 0$. The Lagrangian ap-

proach is very powerful and it can easily be generalized to classical field theory and quantum field theory. In this section, we will explore Lattice QCD by constructing a lagrangian for the strong force and then defining it on a discrete spacetime lattice.

Another important concept that we will use in this derivation is that of gauge invariance. The word gauge refers to a lagrangian having redundant degrees of freedom. We can then define a gauge transformation that leaves the lagrangian invariant. Gauge invariance is a key part of all quantum field theories of the forces of nature, like the electromagnetic force and the strong force.

Gauge transformations form Lie groups. The field theory behind the electromagnetic force, quantum electrodynamics, manifests U(1) symmetry. That means that the Lagrangian is invariant under local transformations of the form:

$$\psi(x) \rightarrow e^{-i\theta(x)}\psi \tag{2.3}$$

where the word local refers to the fact that the introduced phase is spacetime dependent.

In QCD, the equivalent Lie group corresponds to an SU(3) symmetry. That means that the fermion fields, which are now vectors with three components, are invariant under transformations of the form:

$$\psi(x) \rightarrow e^{-i\theta(x_a)\frac{\lambda_a}{2}}\psi(x) \tag{2.4}$$

where now λ_a is a set of 3×3 matrices.

Before starting the formulation, we note that we will be working on Euclidean space. Rotating from Minkowski to Euclidean space takes the time t to $-it$. This makes the relative sign between the time component and the space components of the spacetime metric to disappear. Therefore there is no difference between covariant and contravariant vectors in Euclidean space. This seems like an arbitrary decision right now but its benefits for the formulation of Lattice QCD will manifest later.

2.1.2 Lagrangian formulation of Quantum Chromodynamics

Just like in classical field theories, we can describe QCD by defining a Lagrangian and integrating it with respect to time to find the corresponding action of the strong force. The relevant fields are the quark field, the antiquark field and the gluon field:

$$\psi_{\alpha,c}^f(x), \bar{\psi}_{\alpha,c}^f(x), A_\mu(x)_{cd} \quad (2.5)$$

Therefore we can break the action into two separate terms, one for the gluon-quark interactions and one for the gluon-gluon interactions.

To motivate the form of the fermionic action, we can think analogously to the case of a charged particle in an EM field. We can derive the Hamiltonian of a charged particle in an EM field by taking the Hamiltonian of a free particle and making the substitution $p \rightarrow p - eA$:

$$\begin{aligned} H_{free} &= \frac{p^2}{2m} + e\phi \\ H_{EM} &= \frac{(p-eA)^2}{2m} + e\phi \end{aligned} \quad (2.6)$$

where p is the momentum, m is the mass, e is the charge, ϕ is the particle scalar field and A is the vector EM potential.

Since now we have relativistic fermions, we need to start from the Dirac action in Euclidian space and make the equivalent transformation $\partial_\mu \rightarrow \partial_\mu + igA_\mu(x)$, where g is the strong force coupling constant, equivalent to e for EM. We also need to sum over all quark flavors.

$$\begin{aligned} S_{Dirac}[\psi, \bar{\psi}] &= \int d^4x \bar{\psi}(x)(\gamma_\mu \partial_\mu + m)\psi(x) \\ S_f[\psi, \bar{\psi}, A] &= \sum_{f=1}^{N_f} \int d^4x \bar{\psi}^f(x)(\gamma_\mu(\partial_\mu + igA_\mu(x)) + m^f)\psi^f(x) \end{aligned} \quad (2.7)$$

where γ_μ are the Dirac matrices and g is the the coupling constant. Note that we have suppressed the color and Dirac indices .

Just like for EM fields, we require the fermion action to be invariant under a gauge transformation of the form $\psi(x) \rightarrow \Omega(x)\psi(x)$. This means that $D_\mu(x) \equiv \partial_\mu + igA_\mu(x)$ transforms as $D_\mu(x) \rightarrow \Omega(x)D_\mu(x)\Omega(x)^\dagger$.

To construct the gluonic action, again motivated by EM theory, we define

$$\begin{aligned} G_{\mu\nu}(x) &\equiv -i[D_\mu(x), D_\nu(x)] \\ G_{\mu\nu}(x) &= \partial_\mu A_\nu(x) - \partial_\nu A_\mu(x) + i[A_\mu(x), A_\nu(x)] \end{aligned} \quad (2.8)$$

Under gauge transformations, this becomes $G_{\mu\nu}(x) \rightarrow \Omega(x)G_{\mu\nu}(x)\Omega^\dagger(x)$. Note that there is an extra term compared to the electromagnetic field tensor, since $A(x)$ are now matrices in the color space. We can now construct the gluonic action:

$$S_g[A] = \frac{1}{2} \int d^4x \operatorname{tr}_c[G_{\mu\nu}(x)G_{\mu\nu}(x)] \quad (2.9)$$

The trace over color is taken to make the action gauge invariant.

Taking the sum of Eq. 2.7 and Eq. 2.9, we have now the classical action that describes the strong force. For convenience, we can rescale $A \rightarrow \frac{A}{g}$ and write:

$$\begin{aligned} S[\psi, \bar{\psi}, A] &= \sum_{f=1}^{N_f} \int d^4x \bar{\psi}^f(x) (\gamma_\mu (\partial_\mu + iA_\mu(x)) + m^f) \psi^f(x) \\ &\quad + \frac{1}{2g^2} \int d^4x \operatorname{tr}_c[G_{\mu\nu}(x)G_{\mu\nu}(x)] \end{aligned} \quad (2.10)$$

Let's move now to define the theory described by this action on a discrete space-time lattice.

2.1.3 Lattice QCD naive action

Switching to field theory, we are not dealing with operators anymore but with fields that represent infinitely many degrees of freedom since they are defined everywhere in the space time. We can define a 4D lattice of fixed volume with lattice spacing a ,

so that the spacetime vector can only take discrete values:

$$x_\mu = an_\mu, \quad \mu = 0, 1, 2, 3 \quad (2.11)$$

For this to make physical sense, it must be that at the limit as the volume goes to infinity and a goes to zero we recover the continuum field theory.

The analogy between our previous strong force action (Eq. 2.10) and its lattice discretized version is not necessarily straightforward. The logic behind building both of them is the same though. We start with the fermionic action without an external field, so the Dirac action in Euclidean space including the flavors of the quarks is:

$$S_f^{free}[\psi, \bar{\psi}] = \sum_{f=1}^{N_f} \int d^4x \bar{\psi}^f(x) (\gamma_\mu (\partial_\mu + m^f)) \psi^f(x) \quad (2.12)$$

On a lattice, the derivative will no longer be continuous. There is no unique way to discretize a derivative. Both of the following are valid options:

$$\partial_\mu \psi(x) = \frac{\psi(n + \hat{\mu}) - \psi(n)}{a} \quad (2.13)$$

$$\partial_\mu \psi(x) = \frac{\psi(n + \hat{\mu}) - \psi(n - \hat{\mu})}{2a} \quad (2.14)$$

In the limit as $a \rightarrow 0$, Eq. 2.13 gives the continuum derivative up to $O(a)$ corrections, while Eq. 2.14 up to $O(a^2)$ corrections. For that reason, we choose the definition of Eq. 2.14. Our free fermionic action then becomes:

$$S_f^{free}[\psi, \bar{\psi}] = a^3 \sum_{n \in \Lambda} \sum_{f=1}^{N_f} \bar{\psi}^f(n) \left(\sum_{\mu=0}^4 \gamma_\mu \frac{\psi(n + \hat{\mu}) - \psi(n - \hat{\mu})}{2a} + m^f \psi^f(x) \right) \quad (2.15)$$

where a^3 has been added in front to keep the action unitless.

The next step is to impose gauge invariance to the discretized action. Under our usual transformation $\psi(x) \rightarrow \Omega(x)\psi(x)$ and $\bar{\psi}(x) \rightarrow \bar{\psi}(x)\Omega^\dagger(x)$, the first product of

spinors transforms as:

$$\bar{\psi}(n)\psi(n + \hat{\mu}) \rightarrow \bar{\psi}(n)\Omega^\dagger(n)\Omega(n + \hat{\mu})\psi(n + \hat{\mu}) \quad (2.16)$$

To make this invariant, we introduce a gauge field $U_\mu(n)$ between the two spinors that transforms as:

$$U_\mu(n) \rightarrow \Omega(n)U_\mu(n)\Omega(n + \hat{\mu}) \quad (2.17)$$

Similarly, we can squeeze a $U^\dagger(n - \hat{\mu})$ between the two spinors in the second product ($\bar{\psi}(n)\psi(n - \hat{\mu})$). This field will have the transformation property:

$$U_\mu^\dagger(n - \hat{\mu}) \equiv U_{-\mu}(n) \rightarrow \Omega(n)U_{-\mu}(n)\Omega^\dagger(n - \hat{\mu}) \quad (2.18)$$

Because of the directional nature of the U_μ fields, they are called link variables. We can use them to write our discretized, gauge invariant fermionic action as:

$$S_f[\psi, \bar{\psi}, U] = a^3 \sum_{n \in \Lambda} \sum_{f=1}^{N_f} \bar{\psi}^f(n) \left(\sum_{\mu=0}^4 \gamma_\mu \frac{U_\mu(n)\psi(n + \hat{\mu}) - U_{-\mu}(n)\psi(n - \hat{\mu})}{2a} + m^f \psi^f(x) \right) \quad (2.19)$$

In order to be able to recover Eq. 2.7 from Eq. 2.19, as well as to make physical sense of the link variables, we need to establish a relationship between $U_\mu(n)$ and $A_\mu(x)$. The continuum equivalent of the link variable, $U_c(x, x')$, must transform in the same way under gauge transformations:

$$U_c(x, x') \rightarrow \Omega(x)U_c(x, x')\Omega(x') \quad (2.20)$$

A quantity that satisfies this property is the so called gauge transporter:

$$G(x, y) = e^{i \int_{C_{xx'}} A ds} \quad (2.21)$$

where in the exponential we have a path integral from x to x' .

Motivated by that, we define on the lattice:

$$U_\mu(n) = e^{iaA_\mu(n)} \quad (2.22)$$

Taylor expanding Eq. 2.22, we can easily show that Eq. 2.19 recovers Eq. 2.7 up to second order in a .

In order to find the form of the gluonic part of the action, let us now write down the smallest possible loop on the lattice starting from point n and using link variables:

$$U_{\mu\nu}(n) = U_\mu(n)U_\nu(n + \hat{\mu})U_{-\mu}(n + \hat{\mu} + \hat{\nu})U_{-\nu}(n + \hat{\nu}) \quad (2.23)$$

$$U_{\mu\nu}(n) = U_\mu(n)U_\nu(n + \hat{\mu})U_\mu(n + \hat{\mu})^\dagger U_\nu(n)^\dagger \quad (2.24)$$

Using the transformation properties of $U_\mu(n)$ (Eq. 2.17) it is clear that the trace of $U_{\mu\nu}(n)$ is gauge invariant. Let's sum over all possible such loops and define the gluonic action as:

$$S_g[U] = \frac{2}{g^2} \sum_{n \in \Lambda} \sum_{\mu < \nu} \text{Re tr}(\mathbb{1} - U_{\mu\nu}(n)) \quad (2.25)$$

This gives the desired continuum limit of Eq. after Taylor expanding $A_\nu(n + \hat{\mu})$ up to $O(a^2)$ and expanding $U_{\mu\nu}$ using the Baker-Campbell-Hausdorff formula:

$$e^A e^B = e^{A+B+\frac{1}{2}[A,B]+\dots} \quad (2.26)$$

This concludes the formulation of the strong force action on the lattice. Its form is:

$$S[\psi, \bar{\psi}, U] = a^3 \sum_{n \in \Lambda} \sum_{f=1}^{N_f} \bar{\psi}^f(n) \left(\sum_{\mu=0}^4 \gamma_\mu \frac{U_\mu(n)\psi(n + \hat{\mu}) - U_{-\mu}(n)\psi(n - \hat{\mu})}{2a} + m^f \psi^f(x) \right) + \frac{2}{g^2} \sum_{n \in \Lambda} \sum_{\mu < \nu} \text{Re tr}(\mathbb{1} - U_{\mu\nu}(n)) \quad (2.27)$$

This is called the naive lattice action because it does not take account for the

fermion doubling and Fermi statistics. We will resolve that in the section 2.1.5 by introducing the Wilson term, but first we will review the crucial concept of the path integral.

2.1.4 Path integral and observables

In quantum mechanics there are a number of ways to calculate expectation values of observables. For example, if we want to calculate the expectation value of some operator \hat{O} acting on the ground state of a system, we write:

$$\langle 0 | \hat{O} | 0 \rangle = \int \psi_0^*(x) O \psi_0(x) dx \quad (2.28)$$

where $\psi_0(x)$ is the wavefunction of the ground state. This is the Schrodinger approach, but it does not work well in quantum field theory since we are dealing with an infinite number of degrees of freedom.

Another approach is the path integral formulation:

$$\langle 0 | \hat{O} | 0 \rangle = \frac{1}{Z} \int Dx O(x) e^{iS[x]} \quad (2.29)$$

where $Dx \equiv \prod_x dx(t)$ integrates over all possible paths $x(t)$, $S[x]$ is the action that corresponds to the Hamiltonian and $Z = \int Dx e^{iS[x]}$.

The direct equivalent of the path integral formulation in QCD is:

$$\langle \Omega | O[\psi, \bar{\psi}, A] | \Omega \rangle = \frac{1}{Z} \int D\psi D\bar{\psi} DA O[\psi, \bar{\psi}, A] e^{iS[\psi, \bar{\psi}, A]} \quad (2.30)$$

where $|\Omega\rangle$ is the QCD vacuum state, $Z \equiv \int D\psi D\bar{\psi} DA e^{iS}$, O is an observable combination of fields and operators, $D\psi = \prod_{x_\mu} d\psi(x)$, $DA = \prod_{x_\mu} \prod_{\nu=0}^3 dA_\nu(x)$ and S is the QCD action defined in Eq. 2.10.

Before discussing the lattice equivalent, we notice that moving from Minkowski to Euclidean space ($t \rightarrow -it$) switches all the exponentials $e^{iS} \rightarrow e^{-S}$.

Moving to a lattice of discretized spacetime $x_\mu = an_\mu, \mu = 0, 1, 2, 3$ results in the

following changes:

$$D\psi D\bar{\psi} DA \rightarrow \prod_{n_\mu} d\psi(an_\mu) d\bar{\psi}(an_\mu) dU(an_\mu) \quad (2.31)$$

$$S[\psi, \bar{\psi}, A] \rightarrow S[\psi, \bar{\psi}, U] \quad (2.32)$$

where $S[\psi, \bar{\psi}, U]$ is given by Eq. 2.27.

To understand the kind of observables that can be extracted from this formulation let's pick $O[\psi, \bar{\psi}, U] = \chi(t)\chi^\dagger(0)$, where χ^\dagger is the creation operator of a hadron and χ is its annihilation operator. The hadron creation operator is a combination of quark fields and Dirac matrices that creates a state with the quantum numbers of a hadron. More details about this will be given in section 2.2.3. We write:

$$\begin{aligned} \langle \Omega | \chi(t)\chi^\dagger(0) | \Omega \rangle &= \sum_n \langle \Omega | \chi(t) | n \rangle \langle n | \chi^\dagger(0) | \Omega \rangle \\ &= \sum_n \langle \Omega | e^{Ht} \chi(0) e^{-Ht} | n \rangle \langle n | \chi^\dagger(0) | \Omega \rangle \\ &= \sum_n |\langle n | \chi^\dagger | \Omega \rangle|^2 e^{-(E_n - E_\Omega)t} \end{aligned} \quad (2.33)$$

where in the first line we have inserted a complete set of eigenstates of the hamiltonian and in the second line we have used the time evolution of the operator χ in the Heisenberg picture. In the final result, $\langle n | \chi^\dagger | \Omega \rangle$ is non zero when only $|n\rangle$ is a state with the quantum numbers of the ground or excited states of the hadron, $|h\rangle$, $|h'\rangle$ etc. Using that and setting the vacuum energy $E_\Omega = 0$ we get:

$$\langle \Omega | \chi(t)\chi^\dagger(0) | \Omega \rangle = |\langle h | \chi^\dagger | \Omega \rangle|^2 e^{-E_0 t} + |\langle h' | \chi^\dagger | \Omega \rangle|^2 e^{-E_1 t} + \dots \quad (2.34)$$

As $t \rightarrow \infty$, only the energy of the ground state becomes relevant:

$$\lim_{t \rightarrow \infty} \langle \Omega | \chi(t)\chi^\dagger(0) | \Omega \rangle = |\langle h | \chi^\dagger | \Omega \rangle|^2 e^{-E_0 t} \quad (2.35)$$

As shown before, we can write the left hand side of Eq. 2.35 as a path integral on

the lattice. We can therefore extract the ground state energy of the hadron looking at the exponential decay of the correlator as $t \rightarrow \infty$. Note that in Euclidean space t is not the physical time, just a useful mathematical tool that enables our formulation.

2.1.5 Fermi statistics and the Wilson term

The fermion term of the lattice action involves fermionic fields and thus one needs to make sure that the formulation obeys the Pauli exclusion principle: no two fermions can occupy the same quantum state. This requires that the total wavefunction is antisymmetric under the interchanges of quantum numbers of the fields. The fermionic and antifermionic fields can then be described as Grassman variables, $\eta_i, \bar{\eta}_i$, that satisfy anticommuting properties:

$$\eta_i \eta_j = -\eta_j \eta_i, \quad \bar{\eta}_i \bar{\eta}_j = -\bar{\eta}_j \bar{\eta}_i, \quad \eta_i \bar{\eta}_j = -\bar{\eta}_j \eta_i \quad (2.36)$$

An implication of Grassmanian algebra is the following identity, also known as Wick's theorem:

$$\begin{aligned} \langle \eta_{i_1} \bar{\eta}_{j_1} \dots \eta_{i_m} \bar{\eta}_{j_m} \rangle &= \frac{1}{Z} \int \prod_{k=1}^n d\eta_k d\bar{\eta}_k \eta_{i_1} \bar{\eta}_{j_1} \dots \eta_{i_m} \bar{\eta}_{j_m} e^{\sum_{i,j=1}^n \bar{\eta}_i S_{ij} \eta_j} \\ &= (-1)^n \sum_{P(1, \dots, m)} \text{sign}(P) D_{i_1 j_{P_1}}^{-1} D_{i_2 j_{P_2}}^{-1} \dots D_{i_m j_{P_m}}^{-1} \end{aligned} \quad (2.37)$$

where $P(i_1, \dots, i_N)$ stands for all permutations of i_1, \dots, i_N , $\text{sign}(P)$ for the corresponding sign and Z for the equivalent of a Gaussian integral in Grassmanian algebra, which can be shown to equal:

$$Z = \int d\eta_n d\bar{\eta}_n \dots d\eta_1 d\bar{\eta}_1 e^{\sum_{i,j=1}^n \bar{\eta}_i S_{ij} \eta_j} = \det(S) \quad (2.38)$$

Now let's look back to the lattice path integral, except only considering the

fermionic part of the integral:

$$\langle O \rangle_f = \frac{1}{Z_f} \int \prod_{n_\mu} d\psi(an_\mu) d\bar{\psi}(an_\mu) O[\psi, \bar{\psi}, U] e^{-S_f[\psi, \bar{\psi}, U]} \quad (2.39)$$

where $S_f[\psi, \bar{\psi}, U]$ is the fermionic term of the action:

$$S_f[\psi, \bar{\psi}, U] = a^3 \sum_{n \in \Lambda} \sum_{f=1}^{N_f} \bar{\psi}^f(n) \left(\sum_{\mu=0}^4 \gamma_\mu \frac{U_\mu(n) \psi(n + \hat{\mu}) - U_{-\mu}(n) \psi(n - \hat{\mu})}{2a} + m^f \psi^f(x) \right) \quad (2.40)$$

We can write Eq. 2.40 as a product of the form:

$$a^4 \sum_{n \in \Lambda} \sum_{f=1}^{N_f} \bar{\psi}^f(n) D(n, m) \psi^f(m) \quad (2.41)$$

with:

$$D(n, m) = \sum_{\mu=0}^4 \gamma_\mu \frac{U_\mu(n) \delta_{n+\hat{\mu}, m} - U_{-\mu}(n) \delta_{n-\hat{\mu}, m}}{2a} + m^f \delta_{n, m} \quad (2.42)$$

where we've omitted the Kronecker deltas with color and Dirac indices for simplicity.

Now the form of the fermionic path integral bears great resemblance to the first line of Eq. 2.37, as long as the operator O is a product of fermion fields. The inverse of Eq. 2.42 is then the same as D^{-1} in the second line of Eq. 2.37 up to powers of a . With the aid of Wick's theorem, we have written the path integral in terms of the so called Dirac operator $D(n, m)$.

We now want to investigate how this new quantity behaves in momentum space with a trivial gauge field $U_\mu = 1$. Doing a standard discrete Fourier transformation and inverting the matrix we find:

$$\tilde{D}^{-1}(p) = \frac{m - \frac{i}{a} \sum_\mu \gamma_\mu \sin(p_\mu a)}{m^2 + \frac{1}{a^2} \sum_\mu \sin^2(p_\mu a)} \quad (2.43)$$

In the continuum limit this will give a pole for just one value of p . However on the lattice, the periodicity of the denominator creates multiple unphysical poles, called doublers. This becomes more apparent if one takes the fermion mass to be zero. In

order to remove these poles, we need an extra term, called the Wilson term, in the Dirac operator and, therefore, in the fermionic action.

$$D_{Wilson}(p) = \frac{1}{a} \sum_{\mu} (1 - \cos(p_{\mu}a)) \quad (2.44)$$

Fourier transforming the full Dirac operator, we now get (defining $\gamma_{-\mu} = -\gamma_{\mu}$):

$$D(n, m) = (m + \frac{4}{a})\delta_{n,m} - \frac{1}{2a} \sum_{\mu=\pm 1}^{\pm 4} (1 - \gamma_{\mu})U_{\mu}(n)\delta_{n+\hat{\mu},m} \quad (2.45)$$

where again we have omitted obvious any obvious Kronecker deltas in Dirac and color space.

2.2 Hadron Structure with Lattice Methods

The composite nature of mesons and hadrons creates a lot of questions about their energy spectrum as well as their internal structure. Many possible events can happen inside a hadron; the composite quarks interact with each other via gluons, pairs of quarks and antiquarks are created and annihilated, momentum and charge are distributed in complex ways. In this section we will explore how to shed light into the hadron structure by taking advantage of their interactions through the electromagnetic and the weak force. We will then discuss how one can express and calculate observables on the lattice. For more details we refer the reader to Chapter 3 of *Lattice QCD for Nuclear Physics* and to Chapter 11 of Gattringer & Lang.

2.2.1 Elastic $ep \rightarrow ep$ scattering and the electromagnetic Form Factors

A useful way to study any sorts of particles, from both an experimental and an analytical point of view, is to bombard them with electrons. The way point-like charged particles, like leptons and quarks, interact with the electromagnetic field is well understood from Quantum Electrodynamics. For example, one can implement

the famous Feynman rules to calculate the cross section for the scattering of leptons. For the elastic scattering of electrons off positively charged heavier nuclei, assuming point-like nuclei, one ends up with the Mott cross section:

$$\left(\frac{d\sigma}{d\Omega}\right)_{Mott} = \frac{(Z\alpha)^2 E^2}{4k^2 \sin^4(\theta/2)} \left(1 - \frac{k^2}{E^2} \sin^2(\theta/2)\right) \quad (2.46)$$

where Z is the atomic number, $\alpha = \frac{e^2}{4\pi}$ is the fine structure constant, E is the incident energy, k in the incident momentum and θ is the scattering angle.

If the heavier particle is not a point charge but is described as a spinless charge cloud with normalized charge density $\rho(\mathbf{x})$, it can be shown that the cross scattering becomes:

$$\frac{d\sigma}{d\Omega} = \left(\frac{d\sigma}{d\Omega}\right)_{Mott} |F(\mathbf{q})|^2 \quad (2.47)$$

where $F(\mathbf{q})$ is called the form factor and is the Fourier transform of the charge distribution:

$$F(\mathbf{q}) = \int \rho(\mathbf{x}) e^{i\mathbf{q} \cdot \mathbf{x}} d^3\mathbf{x} \quad (2.48)$$

For a realistic model of elastic $e p$ scattering we take protons to have magnetic spin and take nucleon recoil into consideration. We start with the formula for $e \mu$ scattering in a frame where the muons are initially static.

$$\frac{d\sigma}{d\Omega} = \left(\frac{\alpha^2}{4E^2 \sin^4(\theta/2)}\right) \frac{E'}{E} \left(\cos^2(\theta/2) - \frac{q^2}{2M^2} \sin^2(\theta/2)\right) \quad (2.49)$$

where E' is the energy of the outgoing electron and M is the energy of the muon. To apply this formula to the case of protons, in addition to substituting with the mass of the proton, we need to look back to the matrix transition amplitude that was used for the calculation of the cross section. For the muon case, the lowest order amplitude is:

$$T_{fi} = -i \int j_\mu \left(-\frac{1}{q^2}\right) j^\mu d^4x \quad (2.50)$$

where q is the difference in momentum between the outgoing and the incoming

muon and the transition current is given by

$$j^\mu = -e\bar{u}(k')\gamma^\mu u(k)e^{i(k'-k)x} \quad (2.51)$$

where $u(k)$ stands for the Dirac spinor and γ^μ the Dirac matrices. For the proton case, the second j^μ of Eq. 2.50 must be replaced by a combination of currents that take into consideration the extended structure of the hadron. It turns out that the only two possibilities between the antispinor and spinor of Eq. 2.51 that are Lorentz invariant and independent are γ^μ and $i\sigma^{\mu\nu}q_\nu$, where $\sigma^{\mu\nu} = \frac{i}{2}[\gamma^\mu, \gamma^\nu]$. Therefore we have to multiply with something of the form $[F_1(q^2)\gamma^\mu + \frac{1}{2M}F_2(q^2)i\sigma^{\mu\nu}q_\nu]$. This gives:

$$\frac{d\sigma}{d\Omega} = \left(\frac{d\sigma}{d\Omega}\right)_{Mott} \left[(F_1^2 - \frac{q^2}{4M^2}F_2^2)\cos^2(\theta/2) - \frac{q^2}{2M^2}(F_1 + F_2)^2\sin^2(\theta/2) \right] \quad (2.52)$$

F_1 and F_2 are called the Dirac and Pauli form factors. It is more common to define the Sachs electric and magnetic form factors:

$$\begin{aligned} G_E(Q^2) &= F_1(Q^2) - \tau F_2(Q^2) \\ G_M(Q^2) &= F_1(Q^2) + F_2(Q^2) \end{aligned} \quad (2.53)$$

where $\tau = Q^2/4M^2$ and Q here is the momentum transfer. We rewrite:

$$\frac{d\sigma}{d\Omega} = \left(\frac{d\sigma}{d\Omega}\right)_{Mott} \left[\frac{G_E^2(Q^2) + \tau G_M^2(Q^2)}{1 + \tau} + 2\tau G_M^2(Q^2)\tan^2(\theta/2) \right] \quad (2.54)$$

The relationship between the Sachs electric form factors and the charge distributions is not as straightforward as in the case of the spherical charge cloud (Eq. 2.48). The recoil of the proton makes it hard to relate the two quantities. In a low energy limit though and a frame where no energy is transferred to the proton and it simply recoils back with opposite spatial momentum (the Breit or brick wall frame), we can recover the usual Fourier transform interpretation. The electric form factor can be

written then as:

$$G_E(Q^2) = \int d^3\mathbf{x} e^{i\mathbf{q}\cdot\mathbf{x}} \rho(\mathbf{x}) \simeq 1 - \frac{1}{6}Q^2 \langle r^2 \rangle + \dots \quad (2.55)$$

which lets us define the charge radius as:

$$\langle r^2 \rangle = -6 \left. \frac{dG_E(Q^2)}{dQ^2} \right|_{Q^2=0} \quad (2.56)$$

To sum up, we have taken advantage of elastic ep scattering to express the cross section in terms of the form factors, which in a favorable energy regime are directly related to the charge density and the magnetic moment density of protons and indirectly to the rms radius. As mentioned in the Introduction, there are still inconsistencies in the value of the rms proton radius from different experiments.

Form factors are easy to extract experimentally, as are cross sections. As we will in in section 2.2.4, we can also use lattice techniques to calculate them and consequently provide new information to the proton radius puzzle.

2.2.2 Nucleon decay and the axial Form Factors

Another phenomenon that can be used to shed light to the structure of hadrons is their decay through the weak interaction. The most common and well studied example is the β decay:

$$p \rightarrow n e^+ \nu_e \quad (2.57)$$

$$n \rightarrow p e^- \bar{\nu}_e \quad (2.58)$$

The proton decay can only occur inside a nucleus since it is otherwise energetically unfavorable. The neutron weak decay on the other hand is possible either way and is responsible for the 920 second mean life of neutrons.

Fermi, inspired by the neutron-electron scattering mechanism, proposed that the

invariant amplitude of the beta decay takes the form:

$$\mathcal{M} = G(\bar{u}_n \gamma^\mu u_p)(\bar{u}_{\nu_e} \gamma_\mu u_e) \quad (2.59)$$

where G is known as the Fermi constant. This was a very specific choice and there was no clear reason why the current should only include vector components. Years of experimentation demonstrated without doubt that, in contrast to EM interactions, weak interactions do not conserve parity and there is a directional preference [30]. The neutrino and antineutrino in Eq. 2.57 and Eq. 2.58 are emitted with the sign of their spin projection onto their momentum vector negative and positive respectively. The neutrino is then preferably left-handed and the antineutrino preferably right-handed.

In order to take violation of parity into consideration, it is enough to modify Fermi's proposed current by adding an extra factor of $\frac{1}{2}(1 - \gamma^5)$, where $\gamma^5 = \gamma^1 \gamma^2 \gamma^3 \gamma^4$ in Euclidean space. Simple as it seems, this factor selects the left handed neutrino (or right handed antineutrino) in the β decay interaction. The full current is now called the vector-axial current $V - A$ since it contains a vector term and an axial vector term.

So far we have assumed that protons and neutrons are point particles. Taking their substructure into consideration requires that the coupling constant has some q^2 dependence and also might differ between the two terms of the $V - A$ current. It also introduces additional terms, in fact all possible vector and axial vector terms that leave the amplitude \mathcal{M} Lorentz invariant. For low momentum transfers though, all terms proportional to q can be safely ignored, and thus the matrix element takes the form:

$$\langle p(p', s') | V_\mu - A_\mu | n(p, s) \rangle = \bar{u}_p(p', s') [\gamma_\mu f_1(q^2) - \gamma_\mu \gamma_5 g_1(q^2)] u_n(p, s) \quad (2.60)$$

The quantity $g_A = g_1(0)$ is called the axial charge and is of great importance since it can be experimentally measured but also calculated through lattice techniques, as we will see below.

The conserved vector current hypothesis assumes that under isospin symmetry,

the vector part of the $V - A$ current is the same as the EM vector current. If we focus on the axial vector part of the $V - A$ current away from the zero momentum transfer regime, the corresponding matrix element will contain an axial, a pseudoscalar and a tensor term all accompanied by their respective form factors, $G_A(q^2)$, $G_P(q^2)$ and $G_T(Q^2)$. The one we will be most interested in is the axial form factor, $G_A(q^2)$, because of its relation to the axial charge:

$$g_A = G_A(0) \tag{2.61}$$

So far we have talked about the β decay in terms of the weak current interacting with the nucleons. Taking into consideration the substructure of nucleons though, the current is coupling directly to the quarks. The decay of a neutron (udd) into a proton (uud) is actually the decay of a d quark into a u quark via the weak interaction. The coupling axial current is then of the form $\bar{u}\gamma^\mu\gamma^5d$, where u now refers to the up quark and not to the Dirac spinor. Under the isospin symmetry:

$$\langle p | \bar{u}\gamma^\mu\gamma^5d | n \rangle = \langle p | \bar{u}\gamma^\mu\gamma^5u - \bar{d}\gamma^\mu\gamma^5d | p \rangle \tag{2.62}$$

This is a very useful fact for lattice calculations because it means that all disconnected contributions for the nucleon cancel. A more detailed explanation of this will be given in Section 2.2.4.

2.2.3 Hadron correlators at the quark level

Two-point correlation functions

Section 2.1.4 showed how we can express path integrals on the lattice and use them to extract physical quantities, like the ground state energy of a hadron, or equivalently its mass if it is static. We introduced a structure that creates a hadron at time zero and annihilate it at time t . Every type of structure that measures the overlap of an initial state and a final state is called a correlator. This one is the simplest type and

it's called a 2-point function and it is more commonly used in Fourier space:

$$C_2(t, p) = \sum_x e^{-ipx} T_{\beta\alpha} \langle \Omega | T \{ \chi_\alpha(x, t) \bar{\chi}_\beta(0) \} | \Omega \rangle \quad (2.63)$$

where χ_α and $\bar{\chi}_\beta$ are the annihilation and creation operator of a hadron, $T_{\beta\alpha}$ projects the state in Dirac space and $T\{\dots\}$ is the time ordering operator. Note that the full corresponding path integral should include a $\frac{1}{Z}$ factor, an integration over the gauge field U , an exponential factor e^{-S} as well as determinants of the Dirac operator that arise from the fermionic integral as discussed in Section 2.1.5. The integral over U and the Z factor on a lattice are included by calculating the observable quantity with many different gauge configurations and by using Monte-Carlo sampling. The inclusion of determinants is extremely costly on a decently sized lattice and so sometimes it can be chosen to set them equal to unity. This method is called the quenched (or valence) approximation. It basically ignores the contributions of the vacuum quark loops and only focuses on the valence quarks, which are the quarks that build up the quantum numbers of the hadron (2 for mesons and 3 for baryons).

There are many choices for the creation operator of each hadron, also called interpolator. The interpolator has to combine the quark spins in a correct way in order to give the overall spin of the hadron. It must also combine the quark colors into a color singlet hadron. Finally, it must transform in the same way as the hadron transforms, representing a scalar, pseudoscalar, vector, axial vector or tensor. Taking all these into consideration, one possible choice for the interpolators of the most common hadrons, the pion and the proton, are:

$$\chi_\pi(x) = \bar{d}_\alpha^a(x) \gamma_{\alpha\beta}^5 u_\beta^a(x) \quad (2.64)$$

$$\chi_{p;\alpha}(x) = \epsilon^{abc} (u_\beta^{Ta}(x) (C \gamma^5)_{\beta\gamma} d_\gamma^b(x)) u_\alpha^c(x) \quad (2.65)$$

where u , d and s are the spinors for the up, down and strange quark, ϵ^{abc} is the antisymmetric Levi-Civita tensor and C is the charge conjugation matrix.

We can then write the two-point function for the pion as:

$$C_2(t, p) = \sum_x e^{-ipx} T_{\beta\alpha} \langle \Omega | T \{ \bar{d}_\alpha^a(x) \gamma_{\alpha\beta}^5 u_\beta^a(x) \bar{u}_{\beta'}^{a'}(0) \gamma_{\beta'\alpha'}^5 d_{\alpha'}^{a'}(0) \} | \Omega \rangle \quad (2.66)$$

From Wick's theorem (see Eq. 2.37), the contraction of a quark and antiquark of the same flavor can be written in terms of the inverse Dirac operator, which we will now call a propagator.

$$\langle \psi_\alpha^a(y) \bar{\psi}_\beta^b(x) \rangle = (D_{\alpha\beta}^{ab}(y, x))^{-1} \equiv S_{\psi; \alpha\beta}^{ab}(y, x) \quad (2.67)$$

where ψ is the quark spinor. The propagator is a matrix in spacetime, Dirac space and color space and each of its entries connects a source (x, b, β) with a sink (y, a, α) . It is not feasible to compute the whole matrix for a particular gauge configuration because it would be extremely costly. Instead it is common to calculate a point-to-all propagator that is generated from a fixed point source (x_0, b_0, β_0) :

$$S_{\alpha\beta_0}^{ab_0}(y, x_0) = \sum_{x, b, \beta} (D_{\alpha\beta}^{ab}(y, x))^{-1} \delta(x - x_0) \delta_{bb_0} \delta_{\beta\beta_0} \quad (2.68)$$

which requires the inversion of the Dirac operator.

To optimize the overlap in correlators, it is useful to use an extended (e.g Gaussian) source instead of a point source. This is achieved by a process called smearing. Similarly the propagators can be made to be smeared at their sources or their sinks. For a more detailed explanation of smearing please refer to Section 6.2 of Gattringer & Lang.

With the use of propagators we can now write Eq. 2.66 as:

$$\begin{aligned} C_2(t, p) &= \sum_x e^{-ipx} \gamma_{\beta'\alpha'}^5 S_{d; \alpha'\alpha}^{a'a}(0, x) \gamma_{\alpha\beta}^5 S_{u; \beta\beta'}^{aa'}(x, 0) \gamma_{\beta'\alpha'}^5 \\ &= \sum_x e^{-ipx} \text{trace} \left[\left(S_{d; \beta'\beta}^{a'a}(x, 0) \right)^\dagger S_{u; \beta\beta'}^{aa'}(x, 0) \right] \end{aligned} \quad (2.69)$$

where in the second line we have used the hermiticity relation $\gamma^5 S(0, x) \gamma^5 = S^\dagger(x, 0)$.

The trace of Eq. 2.69 is taken over both the Dirac space and the color space. Under isospin symmetry, the final result contains only one point-to-all propagator of light mass, $S(x, 0)$, and can be readily calculated on the lattice.

Using the same steps we get for the proton:

$$C_2(t, p) = \sum_x e^{-ipx} \epsilon^{abc} \epsilon^{a'b'c'} \text{trace}[(C\gamma^5)_{\beta\alpha} S_{\alpha\alpha'}^{aa'}(x, 0) (C\gamma^5)_{\alpha'\beta'}^T S_{\beta\beta'}^{bb'} \text{trace}_s \{ S_{\gamma\gamma'}^{cc'} T_{\gamma'\gamma} \} \\ - (C\gamma^5)_{\beta'\alpha'} S_{\alpha'\alpha}^{T_s; aa'}(x, 0) (C\gamma^5)_{\alpha\beta}^T S_{\beta\gamma'}^{bc'}(x, 0) T_{\gamma'\gamma} S_{\gamma\beta'}^{cb'}] \quad (2.70)$$

where the s index refers to a trace or transpose in the Dirac space only and $T_{\gamma'\gamma}$ is a spin projection matrix that we can pick (e.g for polarized versus unpolarized protons).

3-point correlation functions

We will now use this approach to express the correlation function for a hadron that is created at time 0, has one of its valence quarks interact with an external current at time t_1 and gets annihilated at time t_2 . This quantity is called a 3-point correlation function. Its general form in momentum space is:

$$C_3(t_2, t_1; p, p') = \sum_{x_2, x_1} e^{-ip'(x_2-x_1)} e^{-ipx_1} T_{\beta\alpha} \langle \Omega | T \{ \chi_\alpha(x_2) \bar{\psi}_\gamma^b(x_1) \Gamma_{\gamma\delta} \psi_\delta^b(x_1) \bar{\chi}_\beta(0) \} | \Omega \rangle \quad (2.71)$$

where ψ is the quark spinor and Γ the interacting current, which is usually a combination of γ matrices (i.e $\gamma_i \gamma_5$ for the axial vector current). Using the interpolator for the pion (Eq. 2.64) for a u-current:

$$C_3(t_2, t_1; p, p') = \sum_{x_2, x_1} e^{-ip'(x_2-x_1)} e^{-ipx_1} \times \\ \langle \Omega | T \{ \bar{d}_\alpha^a(x_2) \gamma_{\alpha\beta}^5 u_\beta^a(x_2) \bar{u}_\gamma^c(x_1) \Gamma_{\gamma\delta} u_\delta^c(x_1) \bar{u}_{\beta'}^{a'}(0) \gamma_{\beta'\alpha'}^5 d_{\alpha'}^{a'}(0) \} | \Omega \rangle \quad (2.72)$$

There are now two different terms that correspond to the possible Wick contrac-

tions of the quark fields.

$$\begin{aligned}
C_3(t_2, t_1; p, p') = & \sum_{x_2, x_1} e^{-ip'(x_2-x_1)} e^{-ipx_1} \times \\
& [-S_{d; \alpha' \alpha}^{a'}(0, x_2) \gamma_{\alpha\beta}^5 S_{u; \beta\gamma}^{ac}(x_2, x_1) \Gamma_{\gamma\delta} S_{u; \delta\beta'}^{ca'}(x_1, 0) \gamma_{\beta'\alpha'}^5 \\
& + S_{d; \alpha' \alpha}^{a'}(0, x_2) \gamma_{\alpha\beta}^5 S_{u; \beta\beta'}(x_2, 0) \Gamma_{\gamma\delta} S_{u; \delta\gamma}^{cc}(x_1, x_1) \gamma_{\beta'\alpha'}^5]
\end{aligned} \tag{2.73}$$

The first term corresponds to the left side of Figure 2-1 and the second term to the right side. The second term contains a loop propagator and is also called disconnected term. Since it is more involved to calculate than non-disconnected terms as well as of lower contribution, it is common to either ignore it or construct combinations of currents that get the term to cancel under isospin symmetry. For the purposes of this project, we will ignore all disconnected terms.

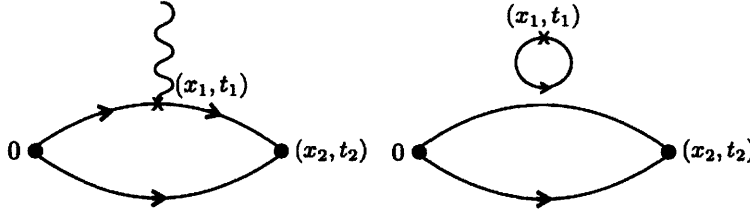


Figure 2-1: Graphical representation of the connected and disconnected term of the pion 3-point function

Continuing with the calculation of the pion 3-point function in terms of quark propagators, we will now drop the u and d indices of the propagators since they are irrelevant due to isospin symmetry. In fact we notice that for the same reason the d -current gives identical result as the u -current for the pion. We also notice that a point-to-all propagator is not enough anymore because of the presence of the $S(x_2, x_1)$ propagator. One can then create two point-to-all propagators, one at the source 0 and one at the sink x_2 . There is another way to go around this though without making two different sources. We write:

$$C_3(t_2, t_1; p, p') = \sum_{x_1} e^{-i(p-p')x_1} \text{trace}[\Sigma_{s; \beta'\gamma}^{a'c}(t_2, x_1, 0; p') \Gamma_{\gamma\delta} S_{\delta\beta'}^{ca'}(x_1, x_0)] \tag{2.74}$$

where Σ_s is called the sequential propagator and is defined as:

$$\Sigma_{s;\beta'\gamma}^{a'c}(t_2, x_1, 0; p') = \sum_{x_2} \Delta_{s;\beta'\beta}^{a'a}(x_2, 0; p') S_{\beta\gamma}^{ac}(x_2, x_1) \quad (2.75)$$

and Δ is called the sequential source and is in the case of the pion:

$$\Delta_{s;\beta'\beta}^{a'a}(x_2, 0; p') = e^{ip'x_2} (S_{\beta'\beta}^{a'a}(x_2, 0))^\dagger \quad (2.76)$$

The reason behind expressing the 3-point function like that is because the way the x_1 and x_2 summations as well as the exponentials are separated allows now to write:

$$\sum_{x_1} D(x_2, x_1) \Sigma_s(t_2, x_1, 0; p') = \Delta_s(x_2, 0; p') \quad (2.77)$$

where $D(x_2, x_1)$ is the Dirac operator. That means that Δ_s acts like a source and we can calculate the sequential propagator Σ_s by solving the above equation for the sequential source. This allows us to avoid making an additional point-to-all propagator at x_2 . It is called the sequential source method and is readily used to calculate the 3-point functions of mesons and baryons. One of its drawbacks is that it fixed the momentum of the sink, requiring and new sequential source for each momentum value used.

We can similarly express the 3-point function of the nucleon in terms of the sequential source propagator. The result in in this case different for the u-current and the d-current. Dropping color and Dirac indices for simplicity, the result is:

$$C_3^{u,d}(t_2, t_1; p, p') = \sum_{x_1} e^{-i(p-p')x_1} \times \text{trace}[\Sigma_s^{u,d}(t_2, x_1, 0; p') \Gamma S(x_1, 0)] \quad (2.78)$$

where the sequential propagator $\Sigma_s^{u,d}$ is now:

$$\Sigma_s^{u,d}(t_2, x_1, 0; p') = \sum_{x_2} \Delta_s^{u,d}(x_2, 0; p') S(x_2, x_1) \quad (2.79)$$

and the sequential sources for the u-current and the d-current equal:

$$\begin{aligned}
\Delta_s^u(x_2, 0; p') &= e^{-ip' x_2} \epsilon^{abc} \epsilon^{a'b'c'} \times [TS(x_2, 0)C\gamma^5 S(x_2, 0)(C\gamma^5)^T \\
&\quad + \text{trace}_s\{TS(x_2, 0)\}C\gamma^5 S(x_2, 0)(C\gamma^5)^T \\
&\quad + \text{trace}_s\{S(x_2, 0)C\gamma^5 S(x_2, 0)(C\gamma^5)^T\}T \\
&\quad + S(x_2, 0)C\gamma^5 S(x_2, 0)(C\gamma^5)^T T]
\end{aligned} \tag{2.80}$$

$$\begin{aligned}
\Delta_s^d(x_2, 0; p') &= e^{-ip' x_2} \epsilon^{abc} \epsilon^{a'b'c'} \times [\text{trace}_s\{TS(x_2, 0)\}(C\gamma^5)^T S(x_2, 0)C\gamma^5 \\
&\quad + TS(x_2, 0)C\gamma^5(C\gamma^5)^T S(x_2, 0)]
\end{aligned} \tag{2.81}$$

T here is again a spin projection matrix that we can pick according to the properties of the nucleon that we want to investigate.

2.2.4 Extracting the form factors from hadron correlators

So far we have seen how to define 2-point and 3-point function on the quark level and how to calculate them on the lattice. Let's now discuss how these correlators are related to hadronic observables like the form factors.

In section 2.1.4 we saw that inserting a complete set of states in a generic hadron 2-point correlator, assuming zero momentum, we can write it as:

$$C_2(t) = \sum_n Z_h^n \bar{Z}_h^n \frac{e^{-m_n t}}{2m_n} \tag{2.82}$$

where m_n are the masses of the hadron channel and Z_h^n (\bar{Z}_h^n) the overlap of the hadron annihilator (creator) states with the different possible eigenstates. Using the same method we can write the 3-point function as:

$$C_3(t, \tau) = \sum_{n,m} Z_h^n \bar{Z}_h^m \frac{e^{-m_n(t-\tau)}}{2m_n} \frac{e^{-m_m \tau}}{2m_m} \langle n | \hat{O} | m \rangle \tag{2.83}$$

where \hat{O} represents the inserted operator (current).

In the limit where $(t - \tau) \rightarrow \infty$ and $\tau \rightarrow \infty$, only the ground state contributions are of interest. Taking then the ratio of the 3-point function to the 2-point function cancels the overlaps and the exponential behavior and it gives direct access to the quantity of interest, $\langle 0 | \hat{O} | 0 \rangle$, the matrix element of the current:

$$\frac{\langle 0 | \hat{O} | 0 \rangle}{2m_0} = \lim_{t-\tau, \tau \rightarrow \infty} \frac{C_3(t, \tau)}{C_2(t)} \quad (2.84)$$

where m_0 is the ground state energy of the hadron at zero momentum, therefore its mass.

As shown in sections 2.2.1 and 2.2.2, this matrix element can be written in terms of form factors. Depending then on the vector \hat{O} that we insert, we can get access to different form factors. For example, setting $\hat{O} = \bar{\psi} \gamma^3 \gamma^5 \psi$ gives us the very useful axial charge:

$$\lim_{t-\tau, \tau \rightarrow \infty} \frac{C_3^{\gamma^3 \gamma^5}(t, \tau)}{C_2(t)} \times 2m_0 = ig_A \quad (2.85)$$

We now have all theoretical tools to measure hadronic observables by calculating 3-point and 2-point functions on the lattice.

2.3 Symanzik Improvement and Renormalization

2.3.1 Clover term

We have shown that the Wilson action gives the QCD action in the continuum limit. However, it is important to make lattice calculations more accurate in discretized space before the continuum limit is taken. In the same way that we chose the symmetric discretized derivative of Eq. 2.14, we can keep adding terms to the action that will increase the accuracy to $O(a^2)$. In addition to the action, we can improve our observables by additional terms. A systematic approach to this is called the Symanzik improvement program.

It can be shown that the Wilson action only needs one additional term for an

$O(a)$ improvement, known as the Pauli term:

$$S_{Pauli} = c_{sw} a^5 \sum_{n \in \Lambda} \sum_{\mu < \nu} \bar{\psi}(n) \frac{1}{2} \sigma_{\mu\nu} \hat{F}_{\mu\nu}(n) \psi(n) \quad (2.86)$$

where c_{sw} is the Sheikholeslami-Wohlert coefficient, $\sigma_{\mu\nu} \equiv \frac{[\gamma_\mu, \gamma_\nu]}{2i}$ and $\hat{F}_{\mu\nu}$ is a discretized form of the field strength tensor. A common choice is:

$$\hat{F}_{\mu\nu}(n) = \frac{-i}{8a^2} (Q_{\mu\nu}(n) - Q_{\nu\mu}(n)) \quad (2.87)$$

where Q is the sum over the rectangular loops of Eq. 2.23:

$$Q_{\mu\nu}(n) \equiv U_{\mu\nu}(n) + U_{\nu-\mu}(n) + U_{-\mu-\nu}(n) + U_{-\nu\mu}(n) \quad (2.88)$$

In the graphical representation of $Q_{\mu\nu}$ the different $U_{\mu\nu}$ look like a clover leaf; for that reason the Pauli term is also called the clover term.

2.3.2 Renormalization of naive currents

In section 2.2 we outlined how to extract hadronic observables using lattice methods. That required the use of different currents, which were inserted in the 3-point functions identical to their continuous forms, γ_μ and $\gamma_\mu \gamma_5$. These currents are not conserved in a discrete lattice though and they are called naive currents. The actual conserved currents are defined to satisfy the Ward identities:

$$\langle 0 | \delta O | 0 \rangle - \langle 0 | O \delta S | 0 \rangle = 0 \quad (2.89)$$

where δ corresponds to the symmetry transformation. Eq. 2.89 is formulated simply by requiring that the expectation value of an operator O is invariant under a symmetry transformation of the fields $\psi \rightarrow \psi + \delta\phi$, $\bar{\psi} \rightarrow \bar{\psi} + \delta\bar{\psi}$. The conserved currents, vector, axial vector, pseudoscalar and tensor, are complicated in form and we will not recite them here. For a full derivation see section 11.1.3 of Gattringer & Lang.

Lattice calculations using conserved currents give matrix elements that correspond

directly to their physical equivalents in the chiral limit. However often the conserved currents are hard to use. In those cases one can use the naive currents and perform renormalization. There are different renormalization schemes depending on the operators in question. For the naive vector current and axial vector current, the renormalization is multiplicative and performed by the factors Z_V and Z_A accordingly. In the chiral limit, $Z_V = Z_A$.

Chapter 3

Method

3.1 Data Acquisition

The data for the 2-point and 3-point functions were acquired using the Chroma library. We constructed a measurement file that performed the following:

- Create a point source at the spatial and temporal origin and smear it.
- Create a propagator starting at the source and smear it at its sink.
- Use the propagator to make sequential sources for the nucleon u-current and the nucleon d-current at timeslices 12, 14 and 16
- Make sequential propagators for all of the above sources.
- Use the propagator from the origin to compute all 2-point contractions.
- Use the propagator from the origin and the sequential propagators to compute all 3-point contractions.

The code was run on a $24^3 \times 64$ lattice of lattice spacing $a \sim 0.12 fm$ and pion mass $m_\pi \approx 0.450 GeV$. We used a total 365 gauge configurations built for two light quarks of equal mass and one heavier. The mass parameter for the heavy s quark corresponded to its physical mass. All propagators were computed for the heavy quark mass.

The action was Symanzik improved with a clover term of clover coefficient 1.249. The type of smearing used was APE smearing.

For the purposes of this project, we will only consider the raw signal and not perform renormalization. Please note that renormalization is necessary before comparing the data with physical results, but since we are operating with a non-physical nucleon any such comparisons are out of our scope. Further calculations at other values of the quark masses would be needed to connect to experiment.

3.2 Data Processing

By the end of the measurements we obtained the correlator functions for $n = 365$ gauge configurations. Given that we only have one dataset but we aim to look at the variability of the mean functions over different possible datasets, we employ the bootstrapping resampling method. $2n$ sets (bootstraps) of n configurations are created randomly with replacement. In each bootstrap we compute the mean of each correlator and then we take the appropriate $\frac{C_3(t,\tau)}{C_2(t)}$ ratios for each timeslice τ . Then we take the average and standard deviation of the ratios over all bootstraps. We also compute the average and standard deviation of $C_2(t)$ for each timeslice, which we will use to estimate the effective mass.

To account for the correlated data, the relevant $\frac{C_3(t,\tau)}{C_2(t)}$ ratios were fitted by minimizing:

$$\chi^2 = \sum_{t,t'=t_{min}}^{t_{max}} (C(t) - A)w(t,t')(C(t') - A) \quad (3.1)$$

with respect to A , where $w(t,t')$ is the inverse of the measured covariance matrix:

$$Cov(t,t') = \frac{1}{m-1} \langle (C(t) - \langle C(t) \rangle)(C(t') - \langle C(t') \rangle) \rangle \quad (3.2)$$

where the averages are taken over the $2n$ bootstraps.

At the first few timeslices the contribution of excited states is too high so we need to tune t_{min} and t_{max} carefully to get a good estimation of the signal plateau. In order to achieve that we start in the middle of the flat signal and we increase the time

interval by one timeslice at a time until $\frac{\chi^2}{d.o.f} > 2$.

After determining the time interval, we fit a constant line to the signal of each bootstrap in order to minimize χ^2 . We average over all bootstraps and determine the variability of the axial factor g_A by calculating the standard deviation of the fitted line.

We use the same process to fit the scaled effective mass, defined as:

$$am_{eff} = \ln \frac{C_2(t)}{C_2(t-1)} \quad (3.3)$$

except in this case we fit a two-parameter exponential $Ae^{-m_{eff}t}$ to the exponentially decaying two-point function.

Taking all results into consideration, we calculate the correctly normalized axial charge for each timeslice t by:

$$g_A(t) = 2m \times \frac{C_3(t, \tau)}{C_2(t)} \quad (3.4)$$

Finally, we extrapolate to $t \rightarrow \infty$ by fitting the values of g_A with a decaying exponential of the form $A + Be^{-Ct}$.

Chapter 4

Results

4.1 Effective mass

The signal of the effective mass of the nucleon, m_{eff} , reached a plateau in the region between timeslices 7 and 14, as shown in Figure 4-1. It was found that:

$$m_{eff} = 0.915 \pm 0.008 \tag{4.1}$$

with a certainty of $\chi^2 = 1.0$.

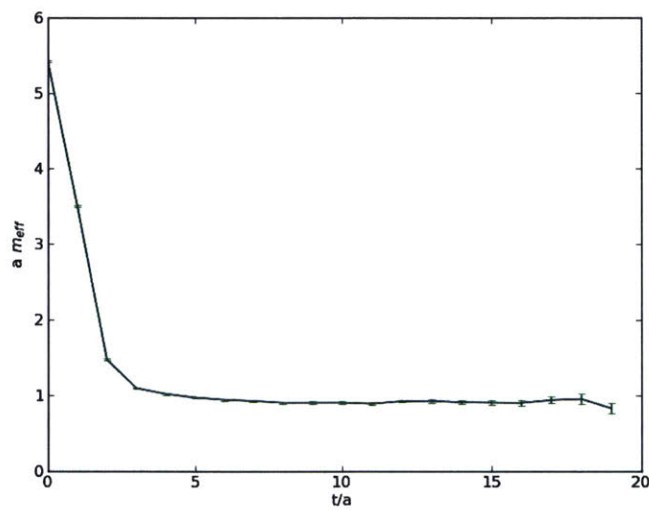


Figure 4-1: Effective mass of nucleon

4.2 Raw signal of g_A

For the dataset with $t_{sink} = 12a$, where a is the lattice constant, the signal reached a plateau between timeslices 3 and 10, with $\chi^2 = 1.0$. The results are presented in Figure 4-2. The value of the non-normalized axial current was found to be:

$$g_A = 0.301 \pm 0.007 \quad (4.2)$$

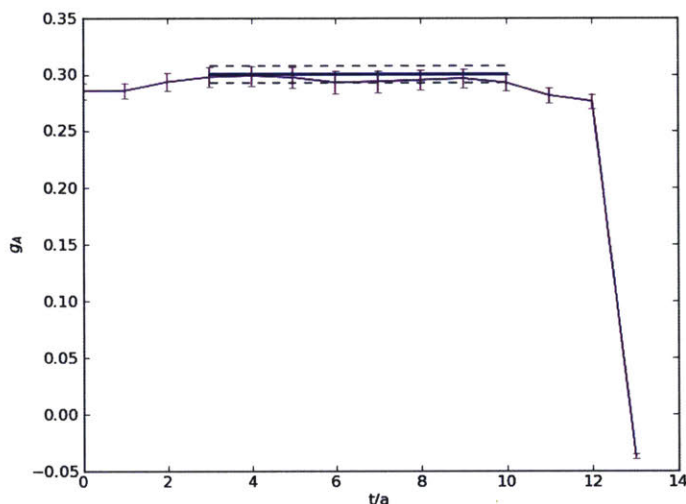


Figure 4-2: Axial charge for $t_{sink} = 12a$

The flat line is the fitted value for g_A and the dashed lines correspond to $g_A \pm \sigma_{g_A}$.

At $t_{sink} = 14a$ the statistical noise of the signal increased significantly, reducing the plateau region from timeslice 3 to 10. For $\chi^2 = 1.3$, the axial current was calculated as:

$$g_A = 0.308 \pm 0.013 \quad (4.3)$$

Last, the signal for $t_{sink} = 16a$ demonstrated higher statistical fluctuations and was fit with a larger than the other two χ^2 value of 1.4 for the region between timeslices 3 and 11. The resulting fit is presented in Figure 4-4. The calculation of g_A gave:

$$g_A = 0.304 \pm 0.015 \quad (4.4)$$

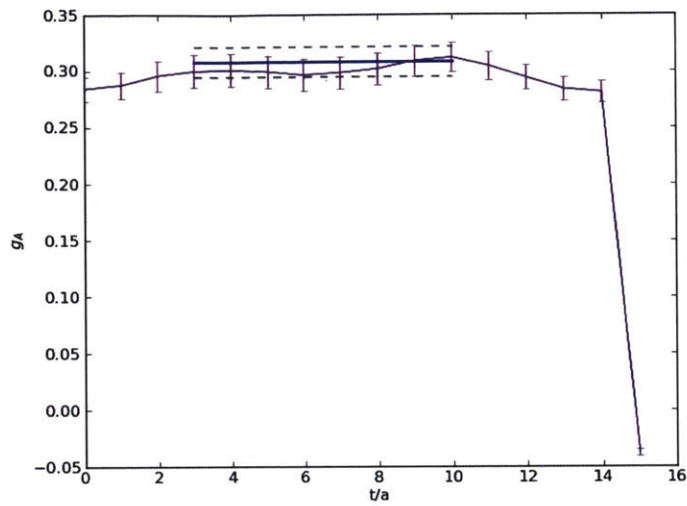


Figure 4-3: Axial charge for $t_{sink} = 14a$

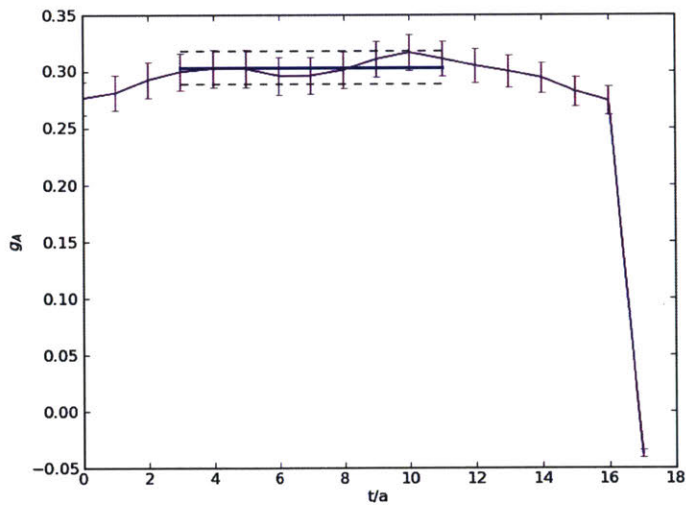


Figure 4-4: Axial charge for $t_{sink} = 16a$

The exponential function fitted to the axial charge values at the different time sinks in order to investigate the behavior at large time scales was of the form $f(t) = 0.558 - 7874e^{-679t}$. It will be discussed further in Chapter 5.

Chapter 5

Conclusion

5.1 Summary of results and discussion

According to Eq. 2.85, to get the correct definition of g_A we need to multiply the result of the raw signal by a factor of the the dimensionless am_{eff} and propagate the errors of the two quantities. The results of the calculation of the naive current axial charge g_A and its error for a heavy nucleon on a $24^3 \times 64$ lattice and fixed sink times 12, 14 and 16 are presented on Table 5.1. We will call the three respective signals 1, 2 and 3. The effective mass of the nucleon was found to be $m_{eff} = 0.915 \pm 0.008$.

Table 5.1: Non-renormalized axial charge g_A of heavy nucleon

Fig.	t_{sink}	g_A	Δg_A	$\Delta g_A\%$
4-2	12	0.551	0.018	3%
4-3	14	0.564	0.029	5%
4-4	16	0.556	0.031	6%

As t_{sink} increases, the signal becomes more irregular and its fluctuations increase. That becomes apparent quantitatively by looking at the increase of the error in the fit; We can also see that qualitatively by inspection of Figures 4-2, 4-3 and 4-4. The fluctuations of the signals at signal 1 and signal 2 look almost symmetrical in the region between timeslices 0-12 and 0-14 respectively. Signal 3 does not demonstrate the same symmetry, making it harder to decide what region should be fit with the χ^2

method.

Even though it was more irregular than the other two, the fitting of signal 3 still gave the relatively low percentage error of 6%. A higher t_{sink} is favorable since excited states contamination is present at small t .

Another thing to consider concerning the results is that the g_A value of signal 1 at the plateau is slightly lower than that of the other two signals. One would expect signal 1 to be closer to the signal 2 than it is to signal 3 since the first two sink times are physically closer and more likely to be affected by similar quantitative effects, like the impact of excited states at lower times. The fluctuations of signals 2 and 3 are higher than those of signal 1 though, giving a possible explanation for this discrepantcy.

The three processed data points and their uncertainties were fitted with an exponential function of the form $A + B e^{-Ct}$ in order to extrapolate to the limit where $t \rightarrow \infty$. The result of the fit was $f(t) = 0.558 - 7874e^{-679t}$.

That implies that at the continuum limit the axial charge approaches the value $g_A = 0.558$. However, since the t_{sinks} used were very close to each other and gave similar values for g_A , it is not clear how accurate this result is. The range of data were of short range and statistically similar to each other, not allowing for a better investigation of how g_A changes with time.

5.2 Suggestions for improvement and future projects

Since the signal for $t_{sink} = 16a$ allows for a fit with a 6% error, it would be interesting to investigate whether the fit improves when we consider a larger number of configurations and of what accuracy would the fit be for a signal with $t_{sink} > 16a$. More data points would allow for a better extrapolation to the continuum limit.

A direct improvement of this project would be to consider processes involving non-zero momentum and different values of momentum insertion in order to estimate the form factor $G_A(q^2)$ as a function of momentum transfer. This could allow for the calculation of the axial charge radius, which is proportional to the derivative of the

axial charge.

One can use the same set-up and configurations to investigate other quantities related to hadron structure, like the electromagnetic form factors, for the proton and other hadrons.

Finally, it would be useful to perform these calculations for lighter quark masses in order to gain a renormalized value for g_A that can be compared with experimental data.

Bibliography

- [1] D. Griffiths. *Introduction to Elementary Particles, Second edition*. WILEY-VCH Verlag GmbH Co. KGaA, 2008. ISBN 978-3-527-40601-2, pages 13-15.
- [2] W.N. Cottingham, D.A. Greenwood. *An Introduction to Nuclear Physics, Second edition*. Cambridge University Press, 2004. ISBN 0-511-03280-3.
- [3] F. Halzen, A.D. Martin. *Quarks and Leptons: An Introductory Course in Modern Particle Physics*, 41-42. John Wiley & Sons, Inc., 1984. ISBN 0-471-88741-2.
- [4] D. Griffiths. *Introduction to Elementary Particles, Second edition*. WILEY-VCH Verlag GmbH Co. KGaA, 2008. ISBN 978-3-527-40601-2, page 19
- [5] G.D. Rochester, C. C. Butler. Evidence for the existence of new unstable elementary particles. *Nature*,160:855-857, 1947.
- [6] V.D Hopper, S. Biswas. Evidence concerting the existence of the new unstable elementary neutral particle. *Phys. Rev.*,80, 1099. doi: 10.1103/PhysRev.80.1099.
- [7] M. Gell-Mann. The interpretation of the particles as displaced charge multiplets. *M. Nuovo Cim*,4:848,1956. doi: 10.1007/BF02748000.
- [8] M. Gell-Mann, Y. Ne'eman. *The eighfold way: a review with a collection of reprints*. W. A. Benjamin, 1964.
- [9] M. Gell-Mann. A Schematic Model of Baryons and Mesons. *Phys. Lett.*,9:214-215, 1964. doi: 10.1016/S0031-9163(64)92001-3.

- [10] G. Zweid. *An $SU(3)$ model for strong interaction symmetry and its breaking.* 1980.
- [11] O.W. Greenberg. Spin and unitary-spin independence in a paraquark model of baryons and mesons. *Phys. Rev. Lett.*, 13:598-602, Nov 1964. doi: 10.1103/PhysRevLett.13.598.
- [12] R. Frish, O. Stern. Uber die magnetische Ablenkung von Wasserstoffmolekullen und das magnetische Moment des Protons. I. *Zeitschrift f \ddot{A} ijr Physik*,85:1, 4-16, 1933. doi: 10.1007/BF01330773
- [13] S.D. Drell, T-M. Yan. Partons and their applications at high energies. *SLAC-PUB-808*, October 1970.
- [14] D.H. Perkins, in: Proceedings of the 16th International Conference on High Energy Physics, National Accelerator Laboratory, Chicago-Batavia, Illinois, September 6-13, 1972, ed. by J.D. Jackson, A. Roberts, Vol. IV.
- [15] D.J. Gross, F. Wilczek. Ultraviolet behavior of non-abelian gauge theories. *Phys. Rev. Lett.*, 30(26):1343-1346, Jun 1973. doi: 10.1103/PhysRevLett.30.1343.
- [16] H.D. Politzer. Reliable perturbative results for strong interactions. *Phys. Rev. Lett.*, 30(26): 1346-1349, Jun 1973. doi: 10.1103/PhysRevLett.30.1346.
- [17] S. Bethke. The 2009 World Average of α_s . *Eur. Phys. J.*, C64:689-703, 2009. doi: 10.1140/epjc/s10052-009-1173-1. arXiv:0908.1135v2 [hep-ph].
- [18] J.E. Augustin *et al.* Discovery of a Narrow Resonance in e^+e^- Annihilation. *Phys. Rev. Lett.*,33, 1406. doi: 10.1103/PhysRevLett.33.1406.
- [19] S.W. Herb *et al.* Observation of a dimuon resonance at 9.6 GeV in 400-GeV proton-nucleus collisions. *Phys. Rev. Lett.*, 39(5):252-255, Aug 1977. doi: 10.1103/PhysRevLett.39.252.
- [20] S. Abachi *et al.* Observation of the top quark. *Phys. Rev. Lett.*, 74(14):2632-2637, Apr 1995. doi: 10.1103/PhysRevLett.74.2632.

- [21] G. Harson *et al.* Evidence for jet structure in hadron production by e^+e^- annihilation. *Phys. Rev. Lett.*, 35(24):1609-1612, Dec 1975. doi: 10.1103/PhysRevLett.351609.
- [22] M. Virchaux, in: 11th International Conference on: Physics in Collision 11, June 20-22, 1991, Colmar, France, ed. by J.-M. Brom, D. Huss, M.-E. Michalon.
- [23] K.G. Wilson. Confinement of quarks. *Phys. Rev. D*, 10(8):2445-2459, Oct 1974. doi: 10.1103/PhysRevD.10.2445.
- [24] C.T.H. Davies. *Lattice QCD*. Institute of Physics Publishing, 2002.
- [25] K.U. Can, A. Kusno, E.V. Mastropas, J.M. Zanotti. Lattice QCD for Nuclear Physics. *Lecture Notes in Physics*, 889:69-70, 2015, ed. by H.-W. Lin, H.B. Meyer. (Springer, Berlin Heidelberg, 2010) doi: 10.1007/978-3-319-08022-2.
- [26] V. Koch. Introduction to Chiral Symmetry. Proceedings of the TASP workshop, Bosen, Germany, Sep 1995. arXiv:nucl-th/9512029v1.
- [27] R.G. Edwards, G.T. Fleming, Ph. Hagler, J.W. Negele, K. Orginos, A.V. Pochinsky, D.B. Renner, D.G. Richards, W. Schroers. Nucleon Axial Charge in Full Lattice QCD. *Phys. Rev. Lett.*, 96, 052001. doi: 10.1103/PhysRevLett.96.052001.
- [28] M. Constantinou. Hadron Structure, in 32st International Symposium on Lattice Field Theory, Jun 23-28 2014, New York, NY. arXiv:1411.0078v1[hep-lat].
- [29] C. Gattringer, C.B. Lang. *Quantum Chromodynamics on the Lattice: An Introductory Presentation*. *Lecture Note in Physics*, 788:284-285. (Springer, Berlin Heidelberg, 2010). doi: 10.1007/978-3-642-01850-3.
- [30] W.N. Cottingham, D.A. Greenwood. *An Introduction to Nuclear Physics, Second edition*. Cambridge University Press, 2004. ISBN 0-511-03280-3. pages 252-253.